

# Single-cell electroporation using proton beam fabricated biochips

S. Homhuan · B. Zhang · F.-S. Sheu · A. A. Bettiol · F. Watt

Published online: 13 February 2012  
© Springer Science+Business Media, LLC 2012

**Abstract** We report the design and fabrication of a novel single cell electroporation biochip featuring high aspect ratio nickel micro-electrodes with smooth side walls between which individual cells are attached. The biochip is fabricated using Proton Beam Writing (PBW), a new direct write lithographic technique capable of fabricating high quality high-aspect-ratio nano and microstructures. By applying electrical impulses across the biochip electrodes, SYTOX® Green nucleic acid stain is incorporated into mouse neuroblastoma (N2a) cells and observed via green fluorescence when the stain binds with DNA inside the cell nucleus. Three parameters; electric field strength, pulse duration, and numbers of pulses have been investigated for the single cell electroporation process. The results indicate high transfection rates as well as cell viability of 82.1 and 86.7% respectively. This single cell electroporation system may represent a promising

method for the introduction of a wide variety of fluorophores, nanoparticles, quantum dots, DNAs and proteins into cells.

**Keywords** Single cell electroporation · Proton beam writing · Biochip

## 1 Introduction

Introduction of biomolecules such as DNA, RNA, proteins, genes and small molecules into target living cells are important in many cell biology experiments.(Kim et al. 2008) For instance, to understand gene function it may be desirable to insert a gene into the cell and remove the proteins resulting from the gene expression from the cell without harming the cell membrane.(Rubinsky 2004) However, the molecules face difficulties penetrating the cell because of barriers caused by the molecular charge, molecular weight, hydrophilicity, or other physio-chemical properties.(Mir and Orłowski 1999) Several methods have been developed to overcome these difficulties, such as using calcium phosphate coprecipitation,(Lee and Welsh 1999) liposome fusion, particle bombardment,(Schmid et al. 1997) viral vectors including retrovirus and adenovirus,(Yin et al. 1998) and electroporation. Among these techniques, electroporation, an electromechanical method of introducing polar molecules into a host cell through the interruption of the cell membrane by a fast and highly localized electric field pulse, is considered a gene delivery tool with a high success rate.(Weaver 2000) Traditionally only the injection methods can target single cells, whereas electroporation has the advantage of being a non-contact method for transient permeabilization of cells.(Olofsson et al. 2003)

Electroporation has been limited in mammalian cells because of technical problems. Conventional cuvette-type multiple cell electroporators have relatively large volumes and hence requires the use of larger amounts of expensive or rare

---

S. Homhuan (✉)  
Prince of Songkla University, Department of Physics,  
Hat Yai,  
Songkhla 90112, Thailand  
e-mail: hsurerat@hotmail.com

A. A. Bettiol · F. Watt  
Centre for Ion Beam Applications, Department of Physics,  
National University of Singapore,  
2 Science Drive 3,  
Singapore 117542, Singapore

B. Zhang  
Department of Biological Science, Faculty of Science, National  
University of Singapore,  
3 Science Drive 4,  
Singapore 117543, Singapore

F.-S. Sheu  
Department of Electrical and Computer Engineering, Nanocore  
Laboratory, Faculty of Engineering, National University of  
Singapore,  
Engineering Drive 1,  
Singapore 117576, Singapore

biomolecules.(Guignet and Meyer 2008) Moreover, as a result of the large spacing between the electrode plates, a high electric field varying from 1 to 12 kV/cm(Neumann et al. 1982; Jamieson et al. 1989; Marti et al. 2004; Tryfona and Bustard 2006) is required at the electrodes in order to get sufficient voltage across each particular cell for molecular penetration into all cells. This high electric field can cause a large portion of cells to be damaged or lysed by an overly high electric field. (Yang et al. 2008) The membrane voltage  $V_m$  induced on a spherical cell of radius  $a$  in an applied field  $E_0$  in its steady state is given by

$$V_m = 1.5aE_0 \cos \theta$$

Where  $\theta$  is the angle between the applied electric field  $E_0$  and the site on the cell membrane at which the potential is determined.(Davalos et al. 2000) From the equation, the voltage across the cell is proportional to the applied electric field, hence, to achieve the transmembrane potential across cell membrane (typical cells are around 0.2–1.5 V (Weaver 1993)), an extremely high electric field is required in between large electrode gap in such conventional electroporation and this cause breakdown of the dielectric layer over the cell membrane as a result of a non-uniform electric field or elevated temperatures during the electroporation process. (Yang et al. 2008)

Several research groups have introduced microelectromechanical systems (MEMS) fabrication techniques to miniaturize the electroporation system hence reducing the spacing distance between the electrodes. At these small dimensions, relatively low potential differences are sufficient to give high electric field strengths in the regions between the electrodes, making it possible, for example, to introduce foreign molecules into cells with voltage as low as 10 V. Another advantage of the miniaturization is that a relatively large area-to-volume ratio in microdevices results in faster heat dissipation per unit surface area. This makes it possible to distinguish between heat and electric field effects.(Huang and Rubinsky 1999; Huang and Rubinsky 2001; Lin and Huang 2001; Lin et al. 2001; Huang and Rubinsky 2003) To achieve efficient electroporation, certain parameters must be optimized. These parameters depend mainly on the pulse of given external fields, such as field strength, pulse duration, and the number of pulses.(Ohshima and Sato 2004) When cells are electroporated, the electric field strength delivered must reach a value that lies within the transmembrane potential range. However, the electric field strength should remain below values which may lead to permanent irreversible damage to cell membrane structure. The field strength range between these two limits is often very narrow.(Tryfona and Bustard 2006) Prolonged shocks or longer pulse durations can also be given to enhance the transport of molecules through the existing pores.(Bilska et al. 2000) Since pulse duration does not appear to increase the cell

surface pore density, the field strength appears to be a more significant contributor to electroporation. The number of pulses also plays an important role in electroporation efficiency. The greater number of pulses, the higher the transformation levels, since more pores will be created in the cell membrane. However, multiple pulses can increase the death rate as overstimulation can lead to apoptosis.

For successful single-cell electroporation, either cells must be isolated from each other, or the electric field focused to target a particular cell.(Nolkrantz et al. 2002) One of the first single-cell electroporation devices was made by Lundqvist (Lundqvist et al. 1998) who studied the electroporation of individual cells using two carbon fiber microelectrodes. These microelectrodes, which had diameters of 5  $\mu\text{m}$ , were moved to within 2–5  $\mu\text{m}$  of the cellular membrane with a micromanipulator. Single cells were selected from a solution and successfully electroporated using 1 volt-millisecond square wave pulses. Although this design demonstrated the possibilities of single-cell electroporation, it is a labor-intensive technique, comparable to existing patch clamp techniques.

Microfluidic electroporation devices.(Lee and Tai 1999; Lin et al. 2001; Suehiro et al. 2003; Gao et al. 2004) are flow-type microchips which can continuously deliver genes, DNAs, or fluorescent stain into cells, and since the flow mechanism eliminates any increase in temperature caused when using a commercial sterile plastic cuvette, then this can improve the survival rate of the electroporated cells.

Other single cell electroporation techniques include: electrolyte-filled capillaries (Nolkrantz et al. 2001), micropipettes (Haas et al. 2001), and atomic force microscopy (AFM) (Nawarathna et al. 2008) based electroporation devices. For electroporation with capillaries and micropipettes (Haas et al. 2001; Nolkrantz et al. 2001), micromanipulators make it possible to obtain high positional probe accuracy. However, since the cells have to be indented thereby creating tension in the membrane, then this method bears a close resemblance to the electroinjection technique. For the AFM method, the AFM tip is moved to make contact with the cell surface before electric pulses are given. This method is capable of performing highly localized electroporation on a single cell surface. However, the tip may disturb and injure cells, and the pulses released from the tip may not be uniform across the cell.

More recently, electroporation has been carried out using microfabricated chips.(Huang and Rubinsky 2001; Khine et al. 2007). Here we present a novel single-cell electroporation biochip which is based on an array of specially designed fixed electrode pairs fabricated using the proton beam writing (PBW) technique. It has been previously shown that on two parallel electrodes the transfection efficiency of the adherent cells (CV-1) was higher than that of the same cells in suspension.(Zheng and Chang 1991) Our design enhances the transfection efficiency of electroporation of fluorescent particles into adherent

cells. The micro-electrode geometry plays an important role in the electroporation process because any non-uniformity of the electric pulses can affect the electroporation efficiency. The PBW technique is employed here to fabricate precise and smooth-sided vertical electrodes, important for creating uniform electric pulses. PBW is a novel direct writing technique utilizing a highly focused beam of fast protons and has been used to pattern precise high aspect ratio structures in suitable materials such as Si, PMMA, SU-8 and HSQ etc. (van Kan et al. 2001) PBW has also been demonstrated as a successful one-step process for direct writing high aspect ratio structures with smooth vertical walls in a relative thick PMMA and SU-8 resist at sub-100 nm resolutions (van Kan et al. 2003). Chiam et al. (Chiam et al. 2007) have studied side wall roughness in structures fabricated in bulk PMMA using proton beam writing. Their results showed that  $R_{rms}$  of less than 7 nm can be achieved using the proton beam writing facility at the Centre for Ion Beam Applications (CIBA), Dept of Physics, National University of Singapore. High aspect ratio electrodes with low roughness side walls, a gap of 50  $\mu\text{m}$  and a height of 7  $\mu\text{m}$  provide the uniform electric pulses for performing high efficiency electroporation.

The prototype biochip was tested by performing electroporation experiments on neuroblastoma N2a cells using SYTOX<sup>®</sup> Green nucleic acid stain. Borate Saline Solution (BSS) (pH 7.4 adjusted with HEPES) was used as the electroporation buffer, because it is suitable for mammalian cell types. SYTOX<sup>®</sup> Green is an excellent green fluorescent nuclear and chromosome counterstain that labels cell with compromised membranes and yields >500-fold fluorescence intensity enhancement upon nucleic acid binding. (Wang and Lu 2006) DEAD Red (ethidium homodimer-2) nucleic acid stain was used to test the viability of cells after electroporation. The

electroporation parameters studied in this work include the amplitude of voltage stimulation, pulse duration and number of pulses applied. We used square wave pulses for all the experiments because they provide *in vitro* experimental conditions resulting in levels of cell survival that cannot be reached using exponentially decaying pulses. (Takahashi et al. 1991)

## 2 Materials and methods

### 2.1 Design, fabrication and experimental set up

Figure 1 is a schematic diagram showing the biochip design. The electrode assembly consists of eight conducting 1800- $\mu\text{m}$ -diameter circular pads, used for external contact with electric probes, connected to the electrodes via 50  $\mu\text{m}$  wide conducting lines. The nickel electrodes, the gaps between which are 50  $\mu\text{m}$ , are fabricated using PBW and subsequent electroplating in order to achieve high aspect ratio and straight-side wall structures. The fabrication process is shown in Fig. 2. A glass cover slip is pre-cleaned with Acetone, Ethanol, and DI water for 10 min successively. Cr is sputtered on the glass slip followed by Au for approximately 10 and 30 nm respectively to form a conductive layer. 7 $\mu\text{m}$  thick Polymethyl methacrylate (495 PMMA A11) is then spin coated on the substrate. The circular contact pads and the conducting lines, for which the geometrical precision is not crucial to the biochip operation, are patterned in the resist layer by standard UV lithography. The electrodes, where higher precision is more critical, are then patterned on the same resist layer by PBW. The sample is then developing in an IPA:DI water (7:3) solution to form the patterns created by both the UV exposure and PBW

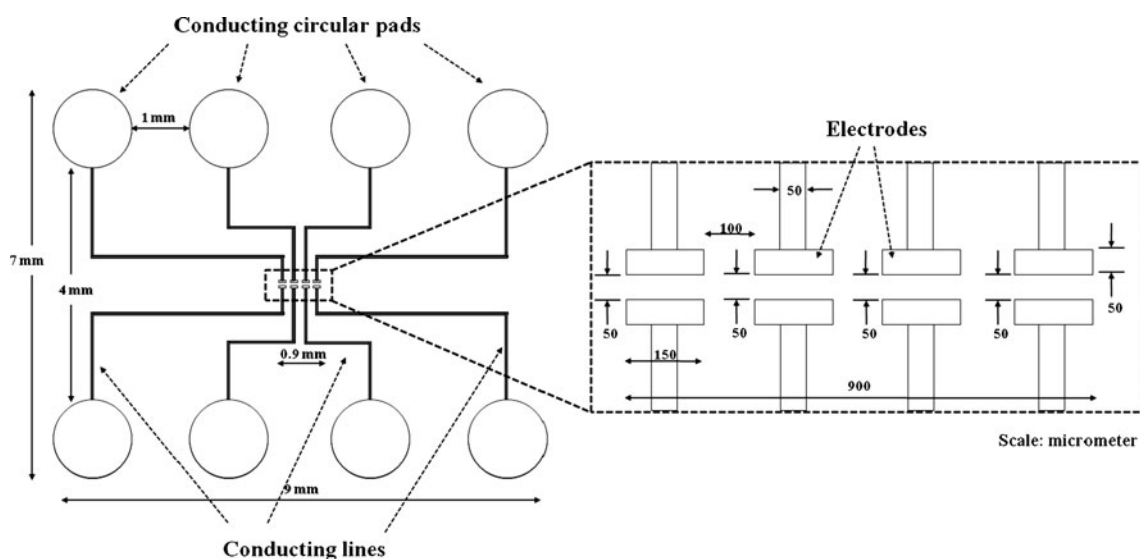


**Fig. 1** Schematic diagram of the prototype chip. The electrode assembly consists of 8 conducting circular shape pads linked to 4 nickel electrode pairs in the centre of the chip. The electroporation experiments are conducted on adherent cells in the electrode gaps

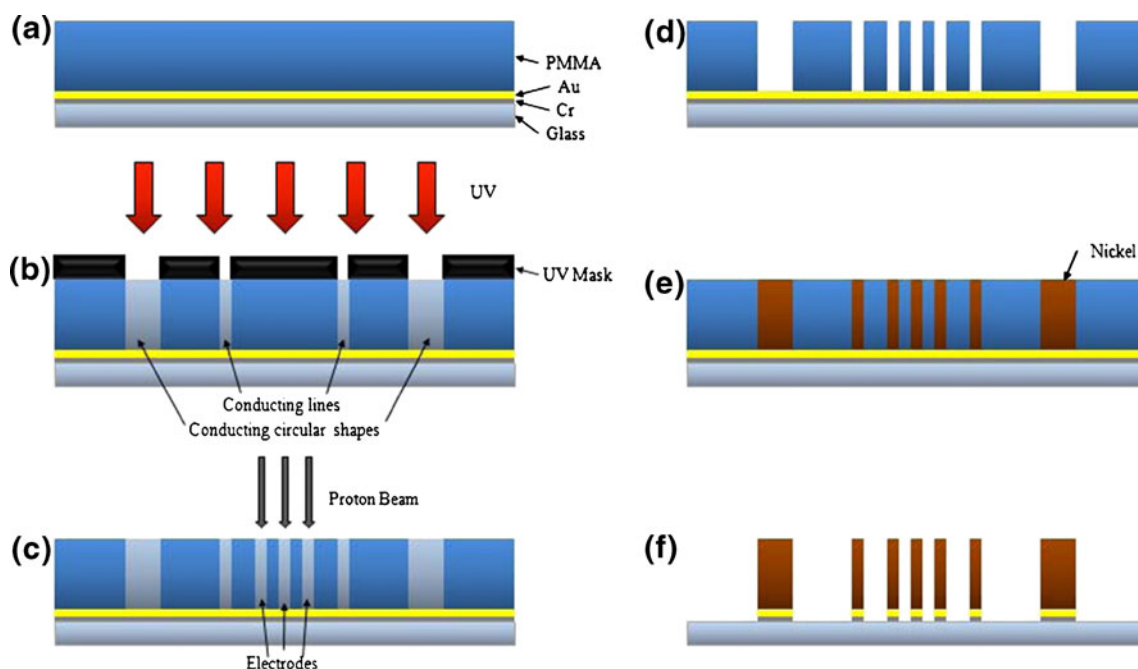


**Fig. 2** Process flow of the biochips fabrication. (a) Cr is sputtered on a glass cover slip followed by Au sputtering for approximately 30 and 10 nm respectively. 7 μm thick PMMA (495 PMMA A11 resist; solids: 11% in Anisole) is then spin coated on the substrate (b) The circular shapes and the conducting lines are patterned by UV lithography. (c)

The electrodes, which require a higher geometric precision, are patterned by PBW to achieve straight side walls and a high aspect ratio. (d) The exposed resist is developed. (e) Nickel is electroplated to form the required metallic electrode assembly. (f) The remaining resist and conductive layer are removed

simultaneously, followed by an Ni electroplating step. Finally, the remaining resists are removed using Toluene revealing the patterned Nickel biochip.

The electric field pulses are generated by a pulse generator (AV-1010-B, Avtech Electrosystems Ltd.) which is controlled by a computer program, and the chip viewed using an inverted microscope (Eclipse TE2000-U, Nikon). The pulses are delivered to the electrodes using two small sharp-tip probes placing in contact with the conducting circular shapes using 3D manipulators.

## 2.2 Experimental procedure

Mouse neuroblastoma N2a cells (ATCC CCL 131, American Type Culture Collection) were grown in Dulbecco's Modified Eagle's medium (DMEM) supplemented with 25 mM HEPES, 10% fetal bovine serum. All cells were propagated in a humidified incubator at 37°C with 5% CO<sub>2</sub>. The cells were then transferred to the chip surface and grown with 2 mL DMEM for 72 h, after which time the chip was 70–80% covered with cells. The DMEM medium was then removed from the chip surface and the chip rinsed with 1 mL BSS. Subsequently, 1 mL of BSS and 50 μL of 500 nM SYTOX<sup>®</sup> Green were then added to the chip.

Since SYTOX<sup>®</sup> Green nucleic acid stain (S7020, 5 mM solution in DMSO, Invitrogen) is a nucleic acid

stain which fluoresces upon binding to DNA but is impermeable to live cells under normal conditions, only those cells which have been successfully electroporated (or alternatively have been killed in the process) will be stained. The electroporation experiments were performed under different electric field parameters, after which the cells were incubated for 30 min to allow for any electroporated SYTOX green stain to bind with the DNA. The stained cells were imaged using the inverted microscope. In order to differentiate between those cells which have been successfully electroporated and those that have died during the process, a second incubation was carried out this time with a cell stain called DEAD Red (ethidium homodimer-2) nucleic acid stain (L7013 component B, 50 μL solution in DMSO, Invitrogen). 50 nM of the DEAD red stain in 1 mL BSS buffer was added to the chip for 30 min. Cells which were successfully electroporated and remained viable exhibited green fluorescence, whilst cells that died during the electroporation subsequently fluoresced red after the addition of the DEAD red stain.

The biochips can be reused for up to 24 times with proper cleaning. First, the chips are trypsinized for 10 min to get rid of all the cells on the surface. The chips are then rinsed with Ethanol, and finally DI water for at least 15 s. Before they are used again for cell culture, the chips have to be exposed with UV light for at least 20 min for sterilisation.

### 3 Results and discussion

#### 3.1 Single-cell electroporation biochip

Figure 3 shows various parts of the electrode assembly: Fig. 3(a) shows a SEM micrograph of one of the electrode pairs, which are 7  $\mu\text{m}$  high with a gap of 50  $\mu\text{m}$ , and 3b indicates the smoothness of the electrode wall edges. Measurements of the sidewall roughness has been previously reported using the process to be 7 nm. (Chiam et al. 2007) Fig. 3(c) and (d) are optical images at different magnifications of the final Nickel electrode assembly.

#### 3.2 Electroporation, and optimal parameters

Two sets of experiments were performed to optimize the percentage of electropermeabilized cells. In the first

$$\text{Transfection rate (\%)} = \frac{\text{Total number of electroporated cells}}{\text{Total number of live cells (before electroporation)}} \times 100$$

$$\text{Viability rate (\%)} = \frac{\text{Total number of live cells (after electroporation)} - \text{Total number of dead cells}}{\text{Total number of live cells (after electroporation)}} \times 100$$

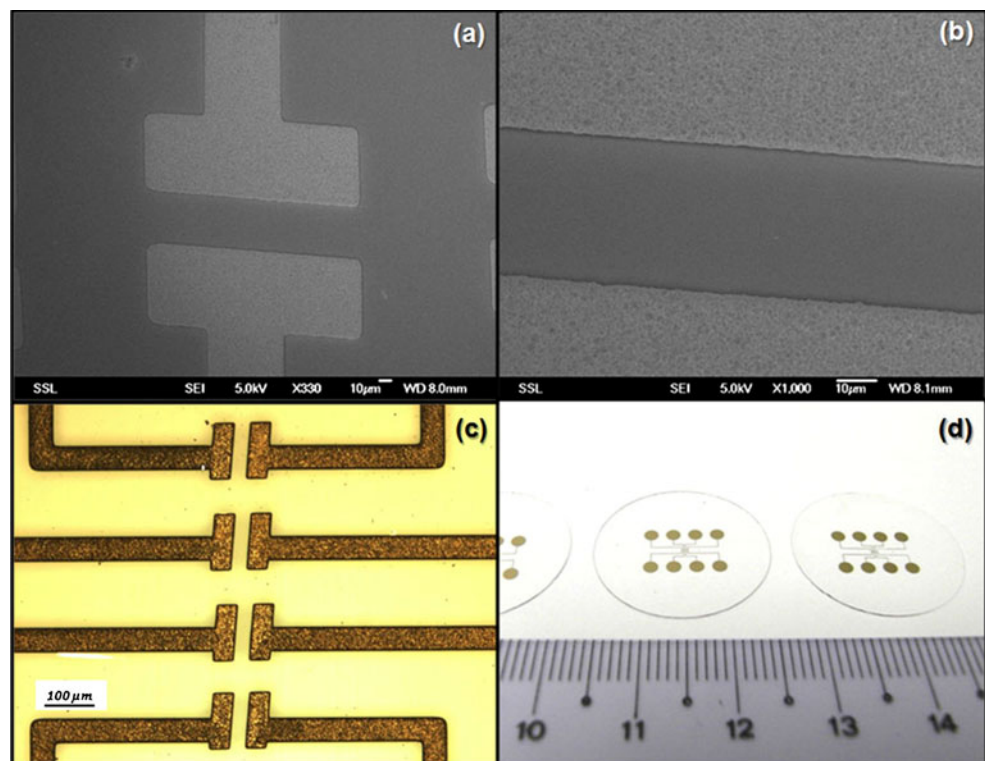
Figure 4 shows examples of successfully transfected cells. Figure 4(a) shows images of cells growing between the electrodes before electroporation was performed. Both

experiment, 20  $\mu\text{L}$  of 500 nM SYTOX<sup>®</sup> Green stain was added to the cells attached between the electrodes, before electroporation. These cells were then subjected to varying electrical parameters (pulse amplitude and number of pulses) and the fluorescent and non-fluorescent cells were counted and their positions recorded. In the second experiment, 20  $\mu\text{L}$  of 50 nM DEAD Red<sup>™</sup> was added 30 min after electroporation was performed to stain the dead cells. Green fluorescence hence serves as an indication that the cells have been successfully electroporated while subsequent red fluorescence indicates that the cells died during the electroporation process. Figure 4 shows the cells (indicated with yellow arrows) that were successfully electroporated, and the cells (indicated with red arrows) that died.

The transfection rate and the viability are given by:

Fig. 4(b) and (c) were taken from the same electrode pair, with different filters (different excitation wavelengths), while Fig. 4(b) was taken 30 min after the electroporation,

**Fig. 3** (a) SEM image of an electrode pair, (b) SEM image of the electrode edge, (c) Optical image of the electrode assembly and (d) Optical image of the completed biochips. The Nickel electrodes are 7  $\mu\text{m}$  high



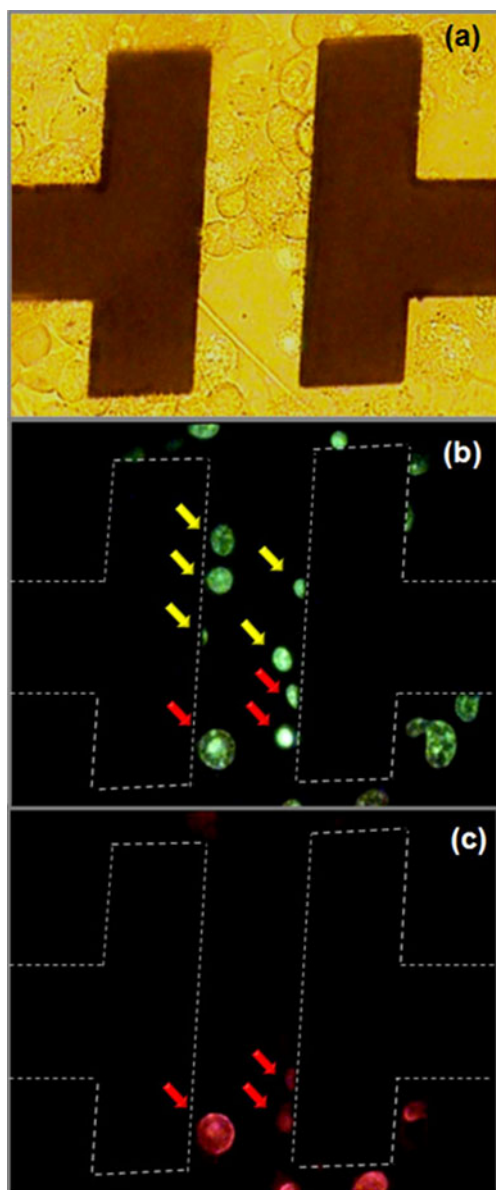
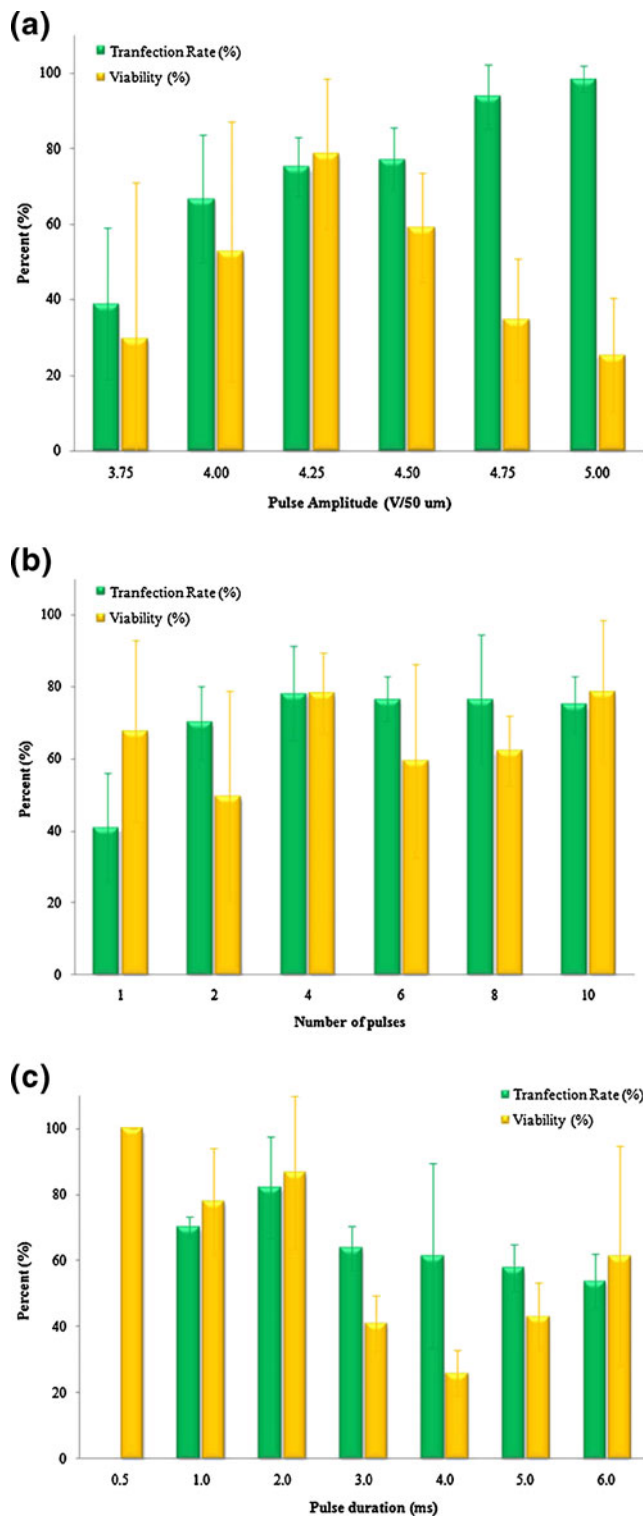


**Fig. 4** Test result from one electroporation experiment. Optical images have been taken using an inverted microscope with 20X magnification. (a) Cells are successfully grown in the gap between a pair of electrodes. (b) Fluorescent image of cells shows green-fluorescent SYTOX® Green stained cells and (c) fluorescent image of cells shows red-fluorescent DEAD Red™ stained cells. (b) and (c) were taken after cells were electroporated with 10 4.25-Volt electric pulses

**Fig. 5** Pulse parameter optimization. (a) Pulse amplitude optimization (3.75, 4.00, 4.25, 4.50, 4.75 and 5.00 V/50  $\mu\text{m}$  with 4 millisecond x 10 pulses). The optimized pulse amplitude is at 4.25 V/50  $\mu\text{m}$ , which gives the highest cell viability with good transfection rate. (b) number of pulses optimization (1, 2, 4, 6, 8 and 10 pulses with 4 millisecond-4.25 V/50  $\mu\text{m}$  pulse). 4 pulses appears optimal for both transfection and viability rates. (c) Pulse duration optimization (0.5, 1.0, 2.0, 3.0, 4.0, 5.0 and 6.0 milliseconds with 4 of 4.25 V/50  $\mu\text{m}$  pulses). A 2 millisecond pulse implies highest transfection rate (82.1%), and viability rate (86.7%), although these data show a wide variability

and Fig. 4(c) was taken 30 min later after the buffer with SYTOX® Green was removed, and the chips incubated with DEAD Red™.

The results for optimal electroporation conditions are shown in Fig. 5. Each data point is the average of 5 experiments, and the error bar is the corresponding standard



deviation. The experiment was performed only when the number of cells between each electrode gap is 5 or more. For pulse amplitude optimization, the experiments were performed with various pulse amplitude (3.74, 4.00, 4.25, 4.50, 4.75 and 5.00 V across 50-micron gap) while number of pulses and pulse duration were fixed at 10 pulses, and 4 millisecond, respectively. The results showed that the highest percentage of cell viability was obtained at 4.25 V, at which a high electroporation rate was also achieved. It was found from previous work that the typical transmembrane potential is in the range of 0.2–1 V mainly depending on size of the cells (Chen et al. 2006). Since N2A cells are about 10  $\mu\text{m}$ , and the optimum pulse amplitude is 4.25 V in 50  $\mu\text{m}$ , the potential across N2A cells is  $\sim 0.85$  V which is in agreement with the theory.

Figure 5(b) shows an optimization of number of pulses when the pulse amplitude and pulse duration were fixed at 4.25 V and 4 milliseconds respectively. The results showed that 4 pulses gave the highest percentage of transfection and cell viability at 78.2 and 78.3% respectively. Figure 5(c) shows an optimization of pulse duration when the pulse amplitude and pulse duration were fixed at 4.25 V and 4 pulses respectively. The results showed that 2-millisecond pulse gave the highest percentage of transfection rate at 82.1%. This rate is high compared to the conventional electroporation techniques which have a transfection rate of 20–50%.

#### 4 Conclusions

A novel electroporation micro-biochip has been successfully fabricated. Each pair of electrodes is spaced 50  $\mu\text{m}$  apart, smaller than in conventional electroporators. The electrode gaps give larger and more uniform electric field distributions, which benefits control of the electroporation process. The use of the PBW technique in the fabrication processes in order to achieve electrodes with high aspect-ratio and straight side walls was also demonstrated. In addition, tests have shown that these biochips can be reused up to 24 times. Studies on neuroblastoma cells on the effects of the pulse amplitudes and the number of pulses were carried out and optimized. Transfection rates of 82.1% and high survival rates of 86.7% were achieved, higher than in most conventional electroporators. The transfection rate and viability for neuroblastoma cells as a function of pulse duration show a large variability in results, indicating that this may be an area where more detailed investigations are necessary. These results demonstrate the feasibility of a fabricating a proton beam written biochip, and indicate that this type of chip may be a promising and efficient tool for introducing impermeant materials, such as drugs, DNA and protein, into individual cells. Since neuroblastoma cells are used as a model system

to study neuronal differentiation (Garcia-Perez et al. 1999), our work could pave the way for the studies of regulation of neural cell development.

**Acknowledgements** We acknowledge the financial support from the Singapore Ministry of Education (MOE) Academic Research Fund under the grant numbers R-144-000-183-112.

#### References

- A.O. Bilska, K.A. DeBruin et al., Theoretical modeling of the effects of shock duration, frequency, and strength on the degree of electroporation. *Bioelectrochemistry* **51**(2), 133–143 (2000)
- C. Chen, S.W. Smye et al., Membrane electroporation theories: a review. *Med. Biol. Eng. Comput.* **44**(1–2), 5–14 (2006)
- S.Y. Chiam, J.A. van Kan et al., Sidewall quality in proton beam writing. *Nucl. Instrum. Methods Phys. Res. B, Beam Interact. Mater. At.* **260**(1), 455–459 (2007)
- R. Davalos, Y. Huang et al., Electroporation: bio-electrochemical mass transfer at the nano scale. *Microscale Thermophys. Eng.* **4**(3), 147–159 (2000)
- J. Gao, X.-F. Yin et al., Integration of single cell injection, cell lysis, separation and detection of intracellular constituents on a microfluidic chip. *Lab on a Chip* **4**(1), 47–52 (2004)
- J. Garcia-Perez, J. Avila et al., Lithium induces morphological differentiation of mouse neuroblastoma cells. *J. Neurosci. Res.* **57**(2), 261–270 (1999)
- E.G. Guignet, T. Meyer, Suspended-drop electroporation for high-throughput delivery of biomolecules into cells. *Nat. Meth.* **5**(5), 393–395 (2008)
- K. Haas, W.C. Sin et al., Single-cell electroporation for gene transfer *in vivo*. *Neuron* **29**(3), 583–591 (2001)
- Y. Huang, B. Rubinsky, Micro-electroporation: improving the efficiency and understanding of electrical permeabilization of cells. *Biomed. Microdevices* **2**(2), 145–150 (1999)
- Y. Huang, B. Rubinsky, Microfabricated electroporation chip for single cell membrane permeabilization. *Sens. Actuators, A* **89**(3), 242–249 (2001)
- Y. Huang, B. Rubinsky, Flow-through micro-electroporation chip for high efficiency single-cell genetic manipulation. *Sens. Actuators, A* **104**(3), 205–212 (2003)
- R.D. Jamieson, M.P. Bodger et al., Transfection by electroporation - cell gene-transfer using electrical impulses, a new process in blood cancer-research. *IEE Proc. Sci. Meas. Tech.* **136**(1), 41–44 (1989)
- M. Khine, C. Ionescu-Zanetti et al., Single-cell electroporation arrays with real-time monitoring and feedback control. *Lab on a Chip* **7**(4), 457–462 (2007)
- J.A. Kim, K.C. Cho et al., A novel electroporation method using a capillary and wire-type electrode. *Biosens. Bioelectron.* **23**(9), 1353–1360 (2008)
- S.-W. Lee, Y.-C. Tai, A micro cell lysis device. *Sens. Actuators, A* **73**(1–2), 74–79 (1999)
- J.H. Lee, M.J. Welsh, Enhancement of calcium phosphate-mediated transfection by inclusion of adenovirus in coprecipitates. *Gene Therapy* **6**(4), 676–682 (1999)
- Y.C. Lin, M.Y. Huang, Electroporation microchips for *in vitro* gene transfection. *J. Micromech. Microeng.* **11**(5), 542–547 (2001)
- Y.C. Lin, C.M. Jen et al., Electroporation microchips for continuous gene transfection. *Sens. Actuators, B* **79**(2–3), 137–143 (2001)
- J.A. Lundqvist, F. Sahlin et al., Altering the biochemical state of individual cultured cells and organelles with ultramicroelectrodes. *Proc. Natl. Acad. Sci. USA* **95**(18), 10356–60 (1998)

- G. Marti, M. Ferguson et al., Electroporative transfection with KGF-1 DNA improves wound healing in a diabetic mouse model. *Gene Therapy* **11**(24), 1780–1785 (2004)
- L.M. Mir, S. Orlowski, Mechanisms of electrochemotherapy. *Adv. Drug Deliv. Rev.* **35**(1), 107–118 (1999)
- D. Nawarathna, K. Unal et al., Localized electroporation and molecular delivery into single living cells by atomic force microscopy. *Appl. Phys. Lett.* **93**(15), 153111–3 (2008)
- E. Neumann, M. Schaeffer et al., Gene-transfer into mouse lymphoma cells by electroporation in high electric-fields. *EMBO J* **1**(7), 841–845 (1982)
- K. Nolkrantz, C. Farre et al., Electroporation of single cells and tissues with an electrolyte-filled capillary. *Anal. Chem.* **73**(18), 4469–4477 (2001)
- K. Nolkrantz, C. Farre et al., Functional screening of intracellular proteins in single cells and in patterned cell arrays using electroporation. *Anal. Chem.* **74**(16), 4300–4305 (2002)
- T. Ohshima, M. Sato, Bacterial sterilization and intracellular protein release by a pulsed electric field. *Recent Progress of Biochemical and Biomedical Engineering in Japan* **I**, 760–760 (2004)
- J. Olofsson, K. Nolkrantz et al., Single-cell electroporation. *Curr. Opin. Biotech.* **14**(1), 29–34 (2003)
- B. Rubinsky, Micro-electroporation in cellomics. *Lab-on-Chips for Cellomics* 123–141 (2004)
- R.M. Schmid, H. Weidenbach et al., Liposome mediated gene transfer into the rat oesophagus. *Gut* **41**(4), 549–556 (1997)
- J. Suehiro, M. Shutou et al., High sensitive detection of biological cells using dielectrophoretic impedance measurement method combined with electroporation. *Sens. Actuators, B* **96**(1–2), 144–151 (2003)
- M. Takahashi, T. Furukawa et al., Gene transfer into human leukemia cell lines by electroporation: experience with exponentially decaying and square wave pulse. *Leuk. Res.* **15**(6), 507–513 (1991)
- T. Tryfona, M.T. Bustard, Enhancement of biomolecule transport by electroporation: a review of theory and practical application to transformation of *Corynebacterium glutamicum*. *Biotechnol. Bioeng.* **93**(3), 413–423 (2006)
- J.A. van Kan, A.A. Bettioli et al., Proton beam micromachining: a new tool for precision three-dimensional microstructures. *Sens. Actuators, A* **92**(1–3), 370–374 (2001)
- J.A. van Kan, A.A. Bettioli et al., Three-dimensional nanolithography using proton beam writing. *Appl. Phys. Lett.* **83**(8), 1629–1631 (2003)
- H.-Y. Wang, C. Lu, Electroporation of mammalian cells in a microfluidic channel with geometric variation. *Anal. Chem.* **78**(14), 5158–5164 (2006)
- J.C. Weaver, Electroporation - a general phenomenon for manipulating cells and tissues. *J. Cell. Biochem* **51**(4), 426–435 (1993)
- J.C. Weaver, Electroporation of cells and tissues. *IEEE Trans. Plasma Sci.* **28**(1), 24–33 (2000)
- S.-C. Yang, K.-S. Huang et al., Determination of optimum gene transfection conditions using the Taguchi method for an electroporation microchip. *Sens. Actuators, B* **132**(2), 551–557 (2008)
- L.H. Yin, S.Q. Fu et al., Results of retroviral and adenoviral approaches to cancer gene therapy. *Stem Cells* **16**(S2), 247–250 (1998)
- Q. Zheng, D.C. Chang, High-efficiency gene transfection by *in situ* electroporation of cultured-cells. *Biochim. Biophys. Acta* **1088**(1), 104–110 (1991)